environmental microbiology

Environmental Microbiology (2019) **21**(4), 1267–1286 doi:10.1111/1462-2920.14527

Metabolic reconstruction of the genome of candidate *Desulfatiglans* TRIP_1 and identification of key candidate enzymes for anaerobic phenanthrene degradation

Ivana Kraiselburd,[1] **Thomas Brüls**,[2,3] **Geronimo Heilmann**,[4] **Farnusch Kaschani**,[4] **Markus Kaiser**[4] **and Rainer U. Meckenstock**[1*]

[1]*Biofilm Centre, Aquatic Microbiology Department, Faculty of Chemistry, University Duisburg-Essen, Essen, Germany.*

[2]*CEA, DRF, Institut Jacob, Genoscope, Evry, France.*

[3]*CNRS-UMR8030, Université Paris-Saclay, Evry, France.*

[4]*Centre of Medical Biotechnology, Chemical Biology Department, Faculty of Biology, University Duisburg-Essen, Essen, Germany.*

Summary

Polycyclic aromatic hydrocarbons (PAHs) are widely distributed pollutants. As oxygen is rapidly depleted in water-saturated PAH-contaminated sites, anaerobic microorganisms are crucial for their consumption. Here, we report the metabolic pathway for anaerobic degradation of phenanthrene by a sulfate-reducing enrichment culture (TRIP) obtained from a natural asphalt lake. The dominant organism of this culture belongs to the *Desulfobacteraceae* family of Deltaproteobacteria and genome-resolved metagenomics led to the reconstruction of its genome along with a handful of genomes from lower abundance bacteria. Proteogenomic analyses confirmed metabolic capabilities for dissimilatory sulfate reduction and indicated the presence of the Embden-Meyerhof-Parnas pathway, a complete tricarboxylic acid cycle as well as a complete Wood-Ljungdahl pathway. Genes encoding enzymes putatively involved in the degradation of phenanthrene were identified. This includes two gene clusters encoding a multisubunit carboxylase complex likely involved in the activation of phenanthrene, as well as genes encoding reductases potentially involved in subsequent ring dearomatization and reduction steps. The predicted metabolic pathways were corroborated by transcriptome and proteome analyses, and provide the first insights into the metabolic pathway responsible for the anaerobic degradation of three-ringed PAHs.

Introduction

Polycyclic aromatic hydrocarbons (PAHs) are widely distributed contaminants with hazardous effects on human health. PAHs are composed of two or more fused aromatic rings and mainly derive from natural gas and petroleum. They are also produced during coal processing and are present in exhaust emissions from vehicles (Cai *et al.,* 2007). Due to their high hydrophobicity and low bioavailability, PAHs are persistent in the environment and recalcitrant to degradation.

Environmental remediation of PAHs is mainly achieved via microbial degradation. Many aerobic bacteria capable of using PAHs as carbon and energy source have been isolated and the corresponding degradation pathways have been widely studied (Peng *et al*., 2008). However, PAH-contaminated aquifers or sediments rapidly become anoxic due to the consumption of oxygen at high carbon loads. Under such conditions, molecular oxygen can be replaced by other electron acceptors for anaerobic respiration, but is critically lacking as a reactive co-substrate for the biochemical activation of hydrocarbons. Anaerobic PAH degradation under iron-reducing, sulfate-reducing and methanogenic conditions has been documented (Meckenstock *et al*., 2016). Nevertheless, very little is known about the responsible organisms or the biochemical mechanisms for PAHs degradation in the absence of molecular oxygen.

Naphthalene ($C_{10}H_8$) is the simplest PAH and has been used as a model compound for studying PAH-degradation. Anaerobic naphthalene degradation proceeds via carboxylation to 2-naphthoate (Mouttaki *et al.,* 2012) followed by formation of the corresponding CoA ester. The further transformation of 2-naphthoyl-CoA occurs via reductive dearomatisation yielding 5,6,7,8-tetrahydro-2-naphthoyl-CoA, which is then reduced in a stepwise

Received 18 July, 2018; accepted 12 December, 2018. *For correspondence. E-mail rainer.meckenstock@uni-due.de; Tel. +49 (0)201 183-6601; Fax +49 (0201) 183-6603.

manner to a hexahydro-2-naphthoyl-CoA (Eberlein *et al.,* 2013a,b; Estelmann *et al.,* 2015).

Knowledge about the anaerobic metabolism of larger PAHs such as the three-ring PAH phenanthrene ($C_{14}H_{10}$) is very scarce. Some information is available on the degradation of phenanthrene under sulfate-reducing conditions. However, neither the genomes nor the degradation pathways have been described. A direct carboxylation of phenanthrene was suggested as a key initial reaction in two of these studies (Zhang and Young 1997; Davidova *et al.,* 2007). Phenanthrene is one of the most abundant compounds present in PAH-contaminated sites, and due to its high toxicity, it is listed as a priority pollutant by the World Health Organization.

A major limitation for studying anaerobic PAH-degradation is the poor bacterial growth. Here, we report on phenanthrene degradation by a sulfate-reducing enrichment culture (TRIP), obtained from the Pitch Lake in Trinidad-Tobago, the world's largest natural asphalt lake. This culture exhibits surprisingly fast growth with phenanthrene as substrate, with generation times of 10 days (Himmelberg *et al*., 2018), offering the unique opportunity to study anaerobic phenanthrene degradation in detail. We describe the key player for phenanthrene degradation by the TRIP culture by genome-resolved metagenomics, as well as the genes and enzymes involved in the anaerobic degradation of this three-ringed PAH.

Results and discussion

The metagenome of the TRIP culture was sequenced, and genome-resolved analyses (Gkanogiannis *et al*., 2016) led to the reconstruction of five nearly-complete genomes that were annotated using the MicroScope microbial genome annotation and analysis platform (Médigue *et al*., 2017; Himmelberg *et al.,* 2018). A general overview of the main genomic features of these organisms is presented in Table 1. The most abundant organism in the TRIP culture accounted for about 60% of the raw reads and was classified as a member of the genus *Desulfatiglans* based on its full length 16S rRNA gene sequence (Fig. 1). This organism showed a close phylogenetic relationship to the naphthalene-degrading Deltaproteobacterial strain NaphS2 (Galushko *et al.,* 1999), but not to 16S rRNA gene clones from the previously described phenanthrene-degrading Phe4 enrichment culture (Davidova *et al.,* 2007; Himmelberg *et al.,* 2018). The other microorganisms of the TRIP culture include another member of the genus *Desulfatiglans*, a *Paludibacter*, as well as members of the family *Spirochaetaceae* and the phylum *Zixibacteria* (Table 1).

In order to evaluate the metabolic potentials of the organisms in the TRIP culture, metabolic pathways were predicted from the genome sequences using the KEGG and MetaCyc databases (Kanehisa and Goto, 2000; Caspi *et al*., 2016), followed by a manual curation to evaluate the completeness of each predicted pathway. Furthermore, expression of the predicted genes was evaluated through a combined metatranscriptomic and metaproteomic analysis of the TRIP culture during growth with phenanthrene. Differential transcriptomic and proteomic analyses were not possible because the TRIP culture is not pure and shifts of the bacterial community were observed upon growth with other substrates (Himmelberg *et al*., 2018).

Previous biochemical studies performed with the TRIP culture suggested that anaerobic phenanthrene degradation involves mechanisms similar to anaerobic naphthalene degradation with an initial carboxylation reaction followed by CoA activation at the carboxyl group and a stepwise reduction of the aromatic rings (Himmelberg *et al.,* 2018). Then, the genes and enzymes involved in the anaerobic degradation of phenanthrene might be similar to those involved in the anaerobic degradation of naphthalene. In order to test this hypothesis, DNA sequences of naphthalene-degradation genes from the Deltaproteobacteria N47 (Bergmann *et al*., 2011a) and NaphS2 (DiDonato *et al*., 2010) were used to search for

Table 1. Overview of the genomes reconstructed from the TRIP metagenome. Phylogenetic classification is based on the full length 16S rRNA gene (SILVA database, Quast *et al*., 2013).

Genome Classification	TRIP_1 *Desulfatiglans*	TRIP_2 *Desulfatiglans*	TRIP_3 *Paludibacter*	TRIP_4 *Spirochaetaceae*	TRIP_5 *Zixibacteria*
Completeness	99.35	99.35	95.61	98.85	99.94
Contamination	1.29	0.97	0.27	0	5.59
Strain heterogeneity	0	0	0	0	0
Length (bases)	5 429 328	4 801 105	3 156 633	2 943 264	3 508 505
GC (%)	47.01	58.62	35.02	55.55	49.72
Number of CDS	4868	4891	2634	2930	3045
Average CDS length (bp)	888	865	1058	944	1039
Average intergenic length (bp)	300	170	149	117	143
Protein coding density (%)	86.92	87.30	90.61	92.32	89.7

Genome completeness was assessed with the CheckM software (Parks *et al.,* 2015). CDS: coding DNA sequence.

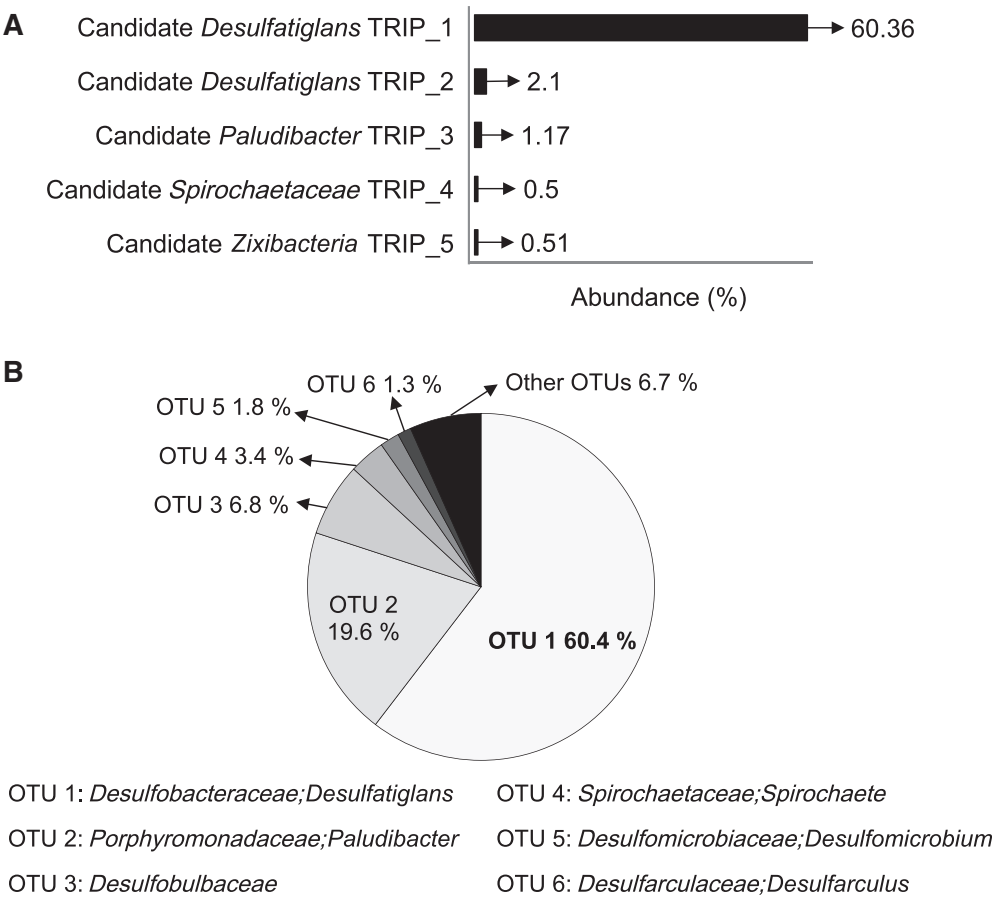

Fig. 1. A. Relative abundance of genomes reconstructed from the TRIP metagenome, calculated by re-mapping raw reads to the assembled scaffolds using the BWA software (Li and Durbin, 2009).
B. Operational taxonomic units (OTU) obtained by clustering 16S rRNA gene amplicon sequences (V3-V4 region) using MetaAmp Version 2.0 (Dong *et al*., 2017).

genes encoding homologous enzymes in the metagenome of the TRIP culture. The pathway for anaerobic naphthalene degradation involves an initial carboxylation step for substrate activation (Mouttaki *et al*., 2012). This step is catalysed by a carboxylase enzyme encoded by a gene cluster containing several *ubiD*-like carboxylase genes both in Deltaproteobacteria N47 and NaphS2 (Bergmann *et al*., 2011a). Two similar gene clusters, encoding a putative phenanthrene carboxylase were found in the genome of candidate *Desulfatiglans* TRIP_1 and the products of those genes were detected during the proteomic and/or transcriptomic analysis (Fig. 2A and Table 2). These results are in concordance with a previously suggested carboxylation as the initial step for the anaerobic degradation of phenanthrene in other bacterial cultures (Zhang and Young 1997; Davidova *et al.,* 2007) and with the carboxylated derivatives of phenanthrene detected during metabolite analyses of the TRIP culture (Himmelberg *et al*., 2018). Moreover, our results provide evidence of the participation of UbiD-like carboxylases in the degradation of three-ring PAHs. The involvement of UbiD-like carboxylases was previously demonstrated not only in the anaerobic degradation of non-substituted PAHs such as naphthalene but also of benzene (Meckenstock *et al.,* 2016).

During anaerobic naphthalene degradation, the produced 2-naphthoic acid is subsequently converted to 2-naphthoyl-CoA by an ATP-dependent 2-naphthoate-CoA ligase (Meckenstock *et al*., 2016). The formation of CoA esters enables further reduction steps and fosters product accumulation within the cell as CoA derivatives cannot permeate through membranes (Fuchs, 2008). The products of five genes of candidate *Desulfatiglans* TRIP_1 displayed between 30% and 33% sequence identity with the proposed 2-naphthoate-CoA ligases of Deltaproteobacteria N47 and NaphS2. Only three of these genes were expressed during growth of the TRIP culture in phenanthrene, and putatively encode phenanthroate-CoA ligases (Table 3(a)). Noteworthy, one of the expressed genes is located in the vicinity of one of the putative carboxylase gene clusters. In Deltaproteobacterium NaphS2, the naphthoyl-CoA ligase gene is located in the vicinity of

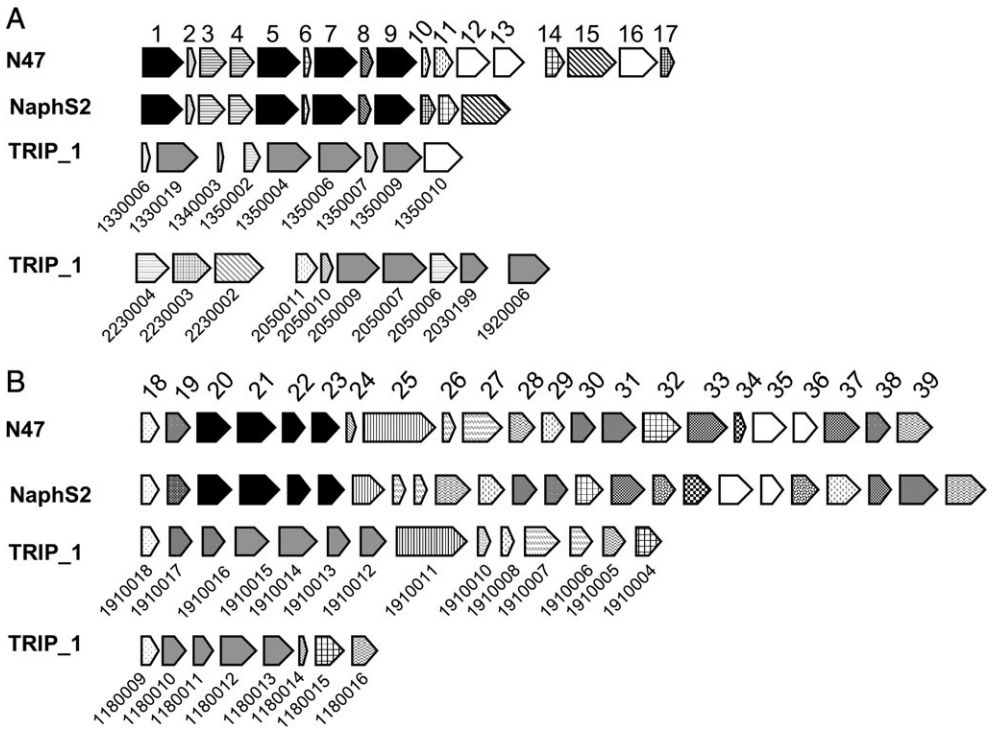

Fig. 2. Genomic organization of the candidate *Desulfatiglans* TRIP_1 gene clusters encoding enzymes potentially involved in phenanthrene carboxylation (A) and in a posterior reduction step (B), based on sequence similarity to genes previously characterized for naphthalene degradation in the Deltaproteobacteria NaphS2 (Di Donato *et al*., 2010) and N47 (Bergmann *et al*., 2011a).
Arrows represent coding DNA sequences (CDS). Products of CDS sharing high percentage of sequence identity (see Tables 2 and 5) between the strains have the same filling patterns within each panel (A and B). The annotated functions of the gene products in Deltaproteobacterium N47 are **1**: putative phenylphosphate carboxylase, alpha subunit; **2**: putative phenylphosphate carboxylase, gamma subunit; **3**: MRP, Fer4_NifH superfamily; **4**: ParA/MinD ATPase like, MRP, Fer4_NifH superfamily; **5**: UbiD family decarboxylase; **6**: conserved hypothetical protein; **7**: UbiD family decarboxylase; **8**: conserved hypothetical protein; **9**: UbiD family decarboxylase; **10** and **11**: HAD hydrolase; **12**: membrane protein involved in aromatic hydrocarbon degradation; **13**: IS4 transposase; **14**: succinate dehydrogenase and fumarate reductase iron–sulfur protein; **15**: putative succinate dehydrogenase flavoprotein subunit; **16**: UbiD family decarboxylase; **17**: pyridoxamine 5′-phosphate oxidase family protein; **18**: TetR-family transcriptional regulato; **19**: enoyl-CoA hydratase/hydrolase/isomerase; **20**, **21**, **22**, **23**: 5,6,7,8-tetrahydro-2-naphthoyl-CoA reductase; **24**: ferredoxin; **25**: oxidoreductase; **26**, **27**: R-β-hydroxyacl-CoA dehydratase MaoC-like; **28**: β-oxoacyl-CoA thiolase; **29**: β-hydroxyacyl-CoA dehydrogenase; **30**, **31**: enoyl-CoA hydratase/hydrolase/isomerase; **32**: metallo-dependant hydrolase; **33**: acyl-CoA dehydrogenase; **34**: CoA-transferase/acetyl-CoA hydrolase; **35**, **36**: acyl-CoA:acetate-lyase AtuA-like; **37**: acyl-CoA dehydrogenase; **38**: enoyl-CoA hydratase/hydrolase/isomerase; **39**: β-oxoacyl-CoA thiolase.

the gene cluster coding for 2-naphthoyl-CoA reductase, the enzyme catalysing the first reduction step of 2-naphthoyl-CoA (DiDonato *et al*., 2010). The genomic neighbourhood of the corresponding gene cluster in candidate *Desulfatiglans* TRIP_1 (see below) contains two genes encoding CoA-transferases, which were expressed during growth on phenanthrene (Table 3(b)). Since some microorganisms are known to use CoA transferases instead of CoA ligases under energy limitations (Meckenstock *et al*., 2016), it is likely that such gene products are involved in this metabolic step. Nevertheless, CoA ligase activity was measured in the TRIP culture through cell-free enzymatic assays (Himmelberg *et al*., 2018). The expressed CoA transferases of candidate *Desulfatiglans* TRIP_1 could also be part of other metabolic pathways. For example, genes encoding these enzymes are part of a synton containing genes involved in butanoate metabolism and fatty acid metabolism (not shown). The third expressed CoA transferase enzyme in candidate *Desulfatiglans* TRIP_1 shares 68% sequence identity with a protein of Deltaproteobacterium NaphS2 involved in late steps of benzoyl-CoA degradation (DiDonato *et al*., 2010).

In Deltaproteobacterium N47, further degradation of 2-naphthoyl-CoA proceeds through consecutive two-electron reduction steps (Eberlein *et al*., 2013a,b; Estelmann *et al*., 2015). The first two steps are catalysed by the enzymes 2-naphthoyl-CoA reductase and 5,6-dihydro-2-naphthoyl-CoA reductase, respectively, both belonging to the 'old yellow enzyme' (OYE) family (Williams and Bruce, 2002). Five genes encoding similar enzymes were found in the genome of candidate *Desulfatiglans* TRIP_1. The combined transcriptome/proteome analysis allowed narrowing down the candidate genes encoding enzymes involved in the reduction of phenanthroyl-CoA. Namely, the products of only two of those genes were detected during the proteomic analysis

Table 2. Gene clusters identified in the genome of candidate *Desulfatiglans* TRIP_1, related to the naphthalene carboxylase gene clusters from the Deltaproteobacteria N47 and NaphS2 (Di Donato *et al*., 2010; Bergmann *et al*., 2011a).

Annotated function in N47	Gene in N47	Gene in NaphS2	Gene in TRIP_1	Annotated function in TRIP_1	Expression (RNA)	Expression (proteins)	Sequence identity with N47/ NapHS2 enzyme (%)
Phenylphosphate carboxylase, α subunit	N47_K27540	NPH_5855	PITCH_v1_a1330019	Phenylphosphate carboxylase, alpha subunit	1160	7	50 (N47_K27540)/(NPH_5855)
Phenylphosphate carboxylase γ subunit	N47_K27530	NPH_5856	PITCH_v1_a1330006	Conserved protein of unknown function	104	5	41 (N47_K27530)/41 (NPH_5856)
MRP, Fer4_NifH superfamily	N47_K27520	NPH_5857	PITCH_v1_a1350002	Conserved protein of unknown function	3921	2	65 (N47_K27520)/64 (N47_K27520)
ParA/MinD ATPase like, MRP, Fer4_NifH superfamily	N47_K27510	NPH_5858	PITCH_v1_a1340003	Protein of unknown function	390	-	61 (N47_K27510)/60 (NPH_5858)
UbiD family carboxylase	N47_K27500	NPH_5859	PITCH_v1_a1350004	3-octaprenyl-4-hydroxybenzoate carboxy-lyase	6752	7	50 (N47_K27500)/50 (NPH_5859)
Conserved hypothetical protein	N47_K27490	NPH_5860	-	-	-	-	-
UbiD family carboxylase	N47_K27480	NPH_5861	PITCH_v1_a1350006	3-octaprenyl-4-hydroxybenzoate carboxy-lyase	10 404	9	53 (N47_K27480)
Conserved hypothetical protein	N47_K27470	NPH_5862	PITCH_v1_a1350007	Conserved protein of unknown function	12 173	-	49 (N47_K27470)
UbiD family carboxylase	N47_K27460	NPH_5863	PITCH_v1_a1350010	Conserved protein of unknown function	2521	32	39 (N47_K27460)
HAD hydrolase	N47_K27450	-	-	-	-	-	-
HAD hydrolase	N47_K27440	-	-	-	-	-	-
Membrane protein (aromatic hydrocarbon degradation)	N47_K27430	-	PITCH_v1_a1350009	Protein of unknown function	3425	-	28 (N47_K27430)
IS4 transposase	N47_K27420	-	-	-	-	-	-
Succinate dehydrogenase/ fumarate reductase iron–sulfur protein	N47_K27410	NPH_5879	-	-	-	-	-
Succinate dehydrogenase flavoprotein subunit	N47_K27400	NPH_5880	-	-	-	-	-
Succinate dehydrogenase flavoprotein subunit	N47_K27390		-	-	-	-	-
Pyridoxamine 5′-phosphate oxidase family protein	N47_K27380	NPH_5878	-	-	-	-	-
Phenylphosphate carboxylase α subunit	N47_K27540	NPH_5855	PITCH_v1_a1920006	Phenylphosphate carboxylase, alpha subunit	64	4	46 (NPH_5855)
Phenylphosphate carboxylase γ subunit	N47_K27530	NPH_5856	-	-			-
MRP, Fer4_NifH superfamily	N47_K27520	NPH_5857	PITCH_v1_a2050011	Conserved protein of unknown function	453	-	66 (N47_K27520)/ 64 (N47_K27520)
ParA/MinD ATPase like, MRP, Fer4_NifH superfamily	N47_K27510	NPH_5858	PITCH_v1_a2050010	Conserved protein of unknown function	330	2	62 (N47_K27510)/61 (NPH_5858)
UbiD family carboxylase	N47_K27500	NPH_5859	PITCH_v1_a2050009	3-octaprenyl-4-hydroxybenzoate carboxy-lyase	390	5	48 (N47_K27500)/59 (NPH_5859)
Conserved hypothetical protein	N47_K27490	NPH_5860	-	-	-	-	-

(Continues)

Table 2. Continued

Annotated function in N47	Gene in N47	Gene in NaphS2	Gene in TRIP_1	Annotated function in TRIP_1	Expression (RNA)	Expression (proteins)	Sequence identity with N47/ NapHS2 enzyme (%)
UbiD family carboxylase	N47_K27480	NPH_5861	PITCH_v1_a2050007	3-octaprenyl-4-hydroxybenzoate carboxy-lyase	254	5	57 (N47_K27480)/54 (NPH_5861)
Conserved hypothetical protein	N47_K27470	NPH_5862	PITCH_v1_a2050006	Conserved protein of unknown function	436	-	50 (N47_K27470)/47 (NPH_5862)
UbiD family carboxylase	N47_K27460	NPH_5863	PITCH_v1_a2230002	UbiD family decarboxylase	720	10	45 (N47_K27460)/47 (NPH_5863)
HAD hydrolase	N47_K27450	-	PITCH_v1_a2030199	HAD hydrolase, family IA, variant 3	548	-	27 (N47_K27450)
HAD hydrolase	N47_K27440	-	-	-	-	-	-
Membrane protein (aromatic hydrocarbon degradation)	N47_K27430	-	-	-	-	-	-
IS4 transposase	N47_K27420	-	-	-	-	-	-
Succinate dehydrogenase/ fumarate reductase iron–sulfur protein	N47_K27410	NPH_5879	PITCH_v1_a2230004	Conserved protein of unknown function	418	9	60 (N47_K27410)/59 (NPH_5879)
Succinate dehydrogenase flavoprotein subunit	N47_K27400	NPH_5880	PITCH_v1_a2230003	Succinate dehydrogenase flavoprotein subunit	426	26	61 (N47_K27400)/63 (NPH_5880)
Succinate dehydrogenase flavoprotein subunit	N47_K27390	-	-	-	-	-	-
Pyridoxamine 5′-phosphate oxidase family protein	N47_K27380	NPH_5878	-	-	-	-	-

Gene expression detected by transcriptome and mass spectroscopy proteome analysis of the TRIP culture grown on phenanthrene are expressed as read counts (fragments per kilobase of gene per million mapped reads) and number of unique peptides identified over runs performed on four independent samples respectively.

Table 3. Aryl-CoA ligase and CoA transferase genes identified in the genome of candidate *Desulfatiglans* TRIP_1, based on homology to previously characterized naphthalene degradation genes in the Deltaproteobacteria N47 and NaphS2 (Di Donato *et al*., 2010; Bergmann *et al*., 2011a).

a

Annotated function in N47	Gene in N47	Gene in NaphS2	Gene in TRIP_1	Annotated function in TRIP_1	Expression (RNA)	Expression (proteins)	Sequence identity with N47/ NapHS2 enzyme (%)
2-naphtoate-coenzyme A ligase	N47_I06840	NPH_5477	PITCH_v1_a1100006	Putative Phenylacetate-coenzyme A ligase	1226	3	31 (N47_I06840)/ 33 (NPH_5477)
			PITCH_v1_a1330026[a]	Putative Phenylacetate-CoA ligase	6008	16	31 (N47_I06840)/ 30 (NPH_5477)
			PITCH_v1_a760031	Putative Phenylacetate-CoA ligase	314	12	31 (N47_I06840)/ 28 (NPH_5477)
			PITCH_v1_a640050	Conserved protein of unknown function	-	-	22 (N47_I06840)/ 21 (NPH_5477)
			PITCH_v1_a1710015	Conserved protein of unknown function	-	-	20 (N47_I06840)/ 22 (NPH_5477)

b

CoA-transferases	PITCH_v1_a420087[b]	Putative Coenzyme A transferase	18 613	20	-
	PITCH_v1_a420086[b]	Putative CoA transferase	17 540	20	-
	PITCH_v1_a920038	CoA-acyltransferase	13 761	11	-

a. In the vicinity of a carboxylase gene cluster.
b. In the vicinity of a reductase gene.
Gene expression detected by transcriptome and mass spectroscopy proteome analysis of the TRIP culture grown on phenanthrene are expressed as read counts (fragments per kilobase of gene per million mapped reads) and number of unique peptides identified over runs performed on four independent samples respectively.

Table 4. Reductase and oxidoreductase genes identified in the genome of candidate *Desulfatiglans* TRIP_1, based on homology to previously characterized naphthalene degradation genes in the Deltaproteobacteria N47 and NaphS2 (Di Donato *et al*., 2010; Bergmann *et al*., 2011a).

a

Annotated function in N47	Gene in N47	Gene in NaphS2	Gene in TRIP_1	Annotated function in TRIP_1	Expression (RNA)	Expression (protein)	Sequence identity with N47/ NapHS2 enzyme (%)
2-naphthoyl-CoA reductase	N47_G38220	NPH_5475 NPH_1753	PITCH_v1_ a190075	NADH-flavin oxidoreductases, Old Yellow Enzyme family	94	17	34 (N47_G38220)/33 (N47_G38210)/36 (NPH_5475)/35 (NPH_1753)/36 (NPH_5476)
			PITCH_v1_ a420108		67	5	35 (N47_G38220)/33 (N47_G38210)/ 36 (NPH_5475)/37 (NPH_1753)/34 (NPH_5476)
5,6-dihydro- 2-naphthoyl-CoA reductase	N47_G38210	NPH_5476	PITCH_v1_ a10001		-	-	31 (N47_G38220)/33 (N47_G38210)/31 (NPH_5475)/32 (NPH_1753)/34 (NPH_5476)
			PITCH_v1_ a1860005		-	-	33 (N47_G38220)/34 (NPH_5475)/35 (NPH_1753)/34 (NPH_5476)
			PITCH_v1_ a1940002		-	-	32 (NPH_1753)/31 (NPH_5476)
			PITCH_v1_ a100001		-	-	33 (NPH_1753)/36 (NPH_5476)

b

NADH-quinone oxidoreductase	N47_G38200	NPH_5472 NPH_5473 NPH_5474 NPH_1750 NPH_1751 NPH_1752	PITCH_v1_ a1090011	NADH dehydrogenase	806	21	52 (NPH_5473)/52 (NPH_1751)
			PITCH_v1_ a1100013	NADH-quinone oxidoreductase	83	4	55 (NPH_5473)/57 (NPH_1751)
			PITCH_v1_ a1120003	NADH-quinone oxidoreductase	232	6	33 (NPH_5474)/34 (NPH_1752)
			PITCH_v1_ a1120005	NADH–ubiquinone oxidoreductase	267	10	56 (N47_G38200)/55 (NPH_5473)/ 56 (NPH_1751)
			PITCH_v1_ a1150094	NADH–ubiquinone oxidoreductase	530	5	37 (NPH_5472)/36 (NPH_1750)/ 31 (NPH_1751)
			PITCH_v1_ a1150095	NADH dehydrogenase	553	20	54 (NPH_5473)/51 (NPH_1751)
			PITCH_v1_ a1430008	4Fe-4S binding domain protein	340	6	53 (NPH_5473)/55 (NPH_1751)
			PITCH_v1_ a1430009	NADH dehydrogenase	120	3	46 (NPH_5472)/46 (NPH_1750)
			PITCH_v1_ a1630007	NADH ubiquinone oxidoreductase	812	22	57 (N47_G38200)/56 (NPH_5473)/57 (NPH_1751)
			PITCH_v1_ a1630008	Benzoyl-CoA reductase	1437	20	42 (NPH_5472)/41 (NPH_1750)

Gene expression detected by transcriptome and mass spectroscopy proteome analysis of the TRIP culture grown on phenanthrene are expressed as read counts (fragments per kilobase of gene per million mapped reads) and number of unique peptides identified over runs performed on four independent samples respectively.

of the TRIP culture (Table 4(a)). The expression of several other genomically clustered oxidoreductase genes was also detected during growth on phenanthrene. These genes bear convincing sequence identities (37%–57%) to the oxidoreductases of Deltaproteobacteria N47 and NaphS2, but unlike the situation in these naphthalene-degrading bacteria, they were not located in the direct vicinity of the putative reductase genes (Table 4(b)).

In the anaerobic degradation of naphthalene, the above-described reactions are followed by a reductive dearomatization step catalysed by the enzyme 5,6,7,8-tetrahydro-2-naphthoyl-CoA reductase, which shows high sequence identity (70%–78%) to class I dearomatizing benzoyl-CoA reductases (Meckenstock *et al*., 2016). In Deltaproteobacteria N47 and NaphS2, the genes encoding this enzyme are surrounded by hydratases, dehydrogenases, hydrolases and thiolases genes, constituting the *thn*-operon. The products of this operon participate in β-oxidation-like reactions following the ring-dearomatisation step (DiDonato *et al*., 2010). Two gene clusters with 45% to 68% product sequence identity to the 5,6,7,8-tetrahydro-2-naphthoyl-CoA reductase of Deltaproteobacterium N47 were identified in the genome of candidate *Desulfatiglans* TRIP_1. The gene clusters in candidate *Desulfatiglans* TRIP_1 also contain other genes with high sequence identity to the *thn-operon* in Deltaproteobacterium N47 (Fig. 2B and Table 5). Products of both gene clusters were detected during the proteome and/or transcriptome analysis of the TRIP culture, providing further evidence for anaerobic degradation of phenanthrene involving reduction and ring dearomatization steps, catalysed by similar enzymes to those involved in the anaerobic degradation of naphthalene. The detection of these reductase genes agrees with the phenanthrene derivatives detected in the TRIP culture showing different degrees of hydrogenation (Himmelberg *et al*., 2018).

Figure 3 shows an overview of the proposed phenanthrene degradation pathway employed by candidate *Desulfatiglans* TRIP_1, including the evidence obtained so far for each reaction at the level of genes, mRNA, proteins, metabolites and enzymatic activity. Interestingly, compared with the genomes of the naphthalene degraders Deltaproteobacteria N47 and NaphS2, the genome of candidate *Desulfatiglans* TRIP_1 contains (and expresses) a higher number of PAH-degradation genes. Considering the higher complexity of phenanthrene, a higher number of enzymatic steps is expected, particularly at the level of aromatic ring reductions.

Genes sharing sequence identities with the aforementioned naphthalene-degradation genes were not found in the other genomes composing the TRIP culture. Considering that the candidate *Desulfatiglans* TRIP_1 is the dominant organism of the TRIP culture, and since potential phenanthrene-degradation genes were only identified in its genome, it is likely that this bacterium is the one responsible for the anaerobic phenanthrene degradation. The fact that the community composition changes upon growth of the TRIP culture with different substrates (Himmelberg *et al*., 2018) further evidences that candidate *Desulfatiglans* TRIP_1 has a major role in the anaerobic degradation of phenanthrene by the TRIP culture.

The genome of candidate *Desulfatiglans* TRIP_1 contains all enzymes needed for dissimilatory sulfate reduction, including ATP sulfurylase (*sat* genes), adenosine-5′-phosphosulfate reductase (*aprAB* genes) and dissimilatory sulfite reductase (*dsrAB* genes) (Fig. 4). This is in concordance with the phylogenetic classification of this organism as well as with the growth of the TRIP culture with sulfate as electron acceptor. It has been proposed for gram negative sulfate-reducing bacteria that electrons are transferred from the quinone pool to DsrAB reductase and AprAB by two different electron transfer complexes: DsrMKJOP together with the protein DsrC, and QmoABC respectively (Pereira *et al.,* 2011). Consistently, genes encoding a DsrMKJOP redox complex are present in the genome of candidate *Desulfatiglans* TRIP_1 and a gene encoding the protein DsrC is located adjacent to the *dsrAB* genes. Moreover, genes close to the *apr* genes are putatively coding for an adenylylsulfate reductase-associated electron transfer protein (*qmoABC* genes). The expression of all of the aforementioned genes was detected by proteomic and/or transcriptomic analyses of the TRIP culture grown with phenanthrene as carbon source (Fig. 4 and Supporting Information Table S1). Unlike some sulfate-reducing bacteria, including the naphthalene-degrading Deltaproteobacterium N47, candidate *Desulfatiglans* TRIP_1 does not carry genes for the reduction of nitrate to ammonium (Bergmann *et al.,* 2011b), in agreement with the inability of the TRIP culture to use nitrate as terminal electron acceptor (Himmelberg *et al*., 2018).

The genome of candidate *Desulfatiglans* TRIP_1 contains all the genes required to run the Embden-Meyerhof-Parnas pathway. Genes encoding the enzymes catalysing the reactions necessary for gluconeogenesis: fructose-1,6-bisphosphatase, phosphoenolpyruvate synthase, pyruvate carboxylase and phosphoenolpyruvate carboxykinase, were also identified in the genome. The expression of these genes was detected by proteomic and/or transcriptomic analyses of the TRIP culture grown on phenanthrene (Fig. 4 and Supporting Information Table S1). The genome of candidate *Desulfatiglans* TRIP_1 also encodes the enzymes for the pentose phosphate pathway. Only the products of genes involved in the non-oxidative branch of this pathway, including transketolase, ribose 5-phosphate isomerase, ribulose-5-phosphate 3-epimerase and a transaldolase were detected in both the transcriptome and proteome analyses (Fig. 4 and Supporting Information

Table 5. Gene clusters related to the tetra-hydro-naphthoyl-CoA reductase operon of Deltaproteobacteria N47 and NaphS2 (Di Donato *et al*., 2010; Bergmann *et al*., 2011a).

Annotated function in N47	Gene in N47	Gene in NaphS2	Gene in TRIP_1	Annotated function in TRIP_1	Expression (RNA)	Expression (proteins)	Sequence identity with N47/ NapHS2 enzyme (%)
TetR-family transcriptional regulator	N47_E41510	NPH_5886	PITCH_v1_a1910018	conserved protein of unknown function	1328	-	41 (N47_E41510)/ 32 (NPH_5886)
Enoyl-CoA hydratase/hydrolase/ isomerase	N47_E41500	NPH_5887	PITCH_v1_a1910016	3-hydroxybutyryl-CoA dehydratase	8194	-	60 (N47_E41500)/41 (N47_E41380)/40 (N47_E41370)/ 57 (NPH_5886)/ 42 (NPH_5907)
5,6,7,8-tetrahydro-2-naphthoyl-CoA reductase	N47_E41490	NPH_5888	PITCH_v1_a1910015	putative benzoyl-CoA reductase, bzd-type, N subunit	6785	30	52 (N47_E41490)/ 55 (NPH_5888)
5,6,7,8-tetrahydro-2-naphthoyl-CoA reductase	N47_E41480	NPH_5889	PITCH_v1_a1910014	putative benzoyl-CoA reductase, bzd-type, O subunit	5685	19	47 (N47_E41480)/ 54 (NPH_5889)
5,6,7,8-tetrahydro-2-naphthoyl-CoA reductase	N47_E41470	NPH_5890	PITCH_v1_a1910013	putative (R)-2-hydroxyglutaryl-CoA dehydratase activator	5459	8	50 (N47_E41470)/ 55 (NPH_5890)
5,6,7,8-tetrahydro-2-naphthoyl-CoA reductase	N47_E41460	NPH_5891	PITCH_v1_a1910012	Benzoyl-CoA reductase, bzd-type, Q subunit	8639	16	68 (N47_E41460)/ 71 (NPH_5891)
Ferredoxin	N47_E41450	-	-	-	-	-	-
Oxidoreductase	N47_E41430	NPH_5892	PITCH_v1_a1910011	BzdV protein	2710	33	43 (N47_E41430)/ 54 (NPH_5892)
R-β-hydroxyacl-CoA dehydratase MaoC-like	N47_E41420	NPH_5893	PITCH_v1_a1910007	conserved protein of unknown function	1259	14	45 (N47_E41420)(40 (NPH_5893)
R-β-hydroxyacl-CoA dehydratase MaoC-like	N47_E41410	NPH_5894	PITCH_v1_a1910006	MaoC-like protein	2272	7	33 (N47_E41420)/ 51 (N47_E41410)/ 55 (NPH_5894)
β-oxoacyl-CoA thiolase	N47_E41400	NPH_5895	PITCH_v1_a1910005	Acetyl-CoA acetyltransferase	4686	25	60 (N47_E41400)/ 32 (N47_E41290)/ 55 (NPH_5895)/ 32 (NPH_5909)
β-hydroxyacyl-CoA dehydrogenase	N47_E41390	NPH_5896	PITCH_v1_a1910008	putative 3-hydroxybutyryl-CoA dehydrogenase	13 225	9	50 (N47_E41390)
Enoyl-CoA hydratase/hydrolase/ isomerase	N47_E41380	NPH_5897	PITCH_v1_a1910016	3-hydroxybutyryl-CoA dehydratase	8194	-	60 (N47_E41500)/41 (N47_E41380)/40 (N47_E41370)/ 57 (NPH_5886)/ 42 (NPH_5907)
Enoyl-CoA hydratase/hydrolase/ isomerase	N47_E41370	NPH_5898	PITCH_v1_a1910017	putative enoyl-CoA hydratase/ isomerase YngF	1711	12	33 (N47_E41380)/ 46 (N47_E41370)/ 48 (NPH_5898)
Metallo-dependant hydrolase (TIM barrel fold)	N47_E41360	NPH_5899	PITCH_v1_a1910004	putative amidohydrolase 2	4116	11	48 (N47_E41360)/ 42 (NPH_5899)
acyl-CoA dehydrogenase	N47_E41350	NPH_5900	-	-	-		-
β-oxoacyl-ACP reductase	-	NPH_5901	PITCH_v1_a1910010	3-oxoacyl-[acyl-carrier-protein] reductase FabG	-	-	56 (NPH_5901)
CoA-transferase / acetyl-CoA hydrolase	N47_E41340	NPH_5902	-	-			-
Acyl-CoA:acetate-lyase AtuA-like	N47_E41330	NPH_5903	-	-			-
Acyl-CoA:acetate-lyase AtuA-like	N47_E41320	NPH_5904	-	-			-
β-oxoacyl-ACP reductase	-	NPH_5905	PITCH_v1_a1910010	3-oxoacyl-[acyl-carrier-protein] reductase FabG	-	10	56 (NPH_5901)
β-hydroxyacyl-CoA dehydrogenase	-	NPH_5906	PITCH_v1_a1910008	putative 3-hydroxybutyryl-CoA dehydrogenase	13 225	9	50 (N47_E41390)
Acyl-CoA dehydrogenase	N47_E41310	NPH_5907	PITCH_v1_a1910016	3-hydroxybutyryl-CoA dehydratase	8194	21	60 (N47_E41500)/41 (N47_E41380)/40 (N47_E41370)/ 57 (NPH_5886)/ 42 (NPH_5907)

Enoyl-CoA hydratase/hydrolase/ isomerase	N47_E41300	NPH_5908	-	-	-	-	-
β-oxoacyl-CoA thiolase	N47_E41290	NPH_5909	PITCH_v1_a1910005	Acetyl-CoA acetyltransferase	4686	25	60 (N47_E41400)/ 32 (N47_E41290)/ 55 (NPH_5895)/ 32 (NPH_5909)
TetR-family transcriptional regulator	N47_E41510	NHP_5886	PITCH_v1_a1180009	Putative Transcriptional regulator, TetR family	1641	-	28 (N47_E41510)/ 28 (NHP_5886)
5,6,7,8-tetrahydro-2-naphthoyl-CoA reductase	N47_E41470	NPH_5890	PITCH_v1_a1180010	Activator of lactoyl-CoA dehydratase	8363	15	45 (N47_E41470)/ 43 (NPH_5890)
5,6,7,8-tetrahydro-2-naphthoyl-CoA reductase	N47_E41460	NPH_5891	PITCH_v1_a1180011	Benzoyl-CoA reductase, bzd-type, Q subunit	7261	12	63 (N47_E41460)/ 60 (NPH_5891)
5,6,7,8-tetrahydro-2-naphthoyl-CoA reductase	N47_E41490	NPH_5888	PITCH_v1_a1180012	Benzoyl-CoA reductase, gamma subunit	10 266	19	46 (N47_E41490)/ 42 (NPH_5888)
5,6,7,8-tetrahydro-2-naphthoyl-CoA reductase	N47_E41480	NPH_5889	PITCH_v1_a1180013	Benzoyl-CoA reductase, beta subunit	10 618	18	36 (N47_E41480)/ 34 (NPH_5889)
Ferredoxin	N47_E41450	-	PITCH_v1_a1180014	Ferredoxin	24 281	-	44 (N47_E41450)
metallo-dependant hydrolase (TIM barrel fold)	N47_E41360	NHP_5899	PITCH_v1_a1180015	Amidohydrolase family protein	20 059	-	60 (N47_E41360)/ 57 (NHP_5899)
β-hydroxyacyl-CoA dehydrogenase	N47_E41390	NPH_5896	PITCH_v1_a1180016	Putative 3-hydroxybutyryl-CoA dehydrogenase	16 175	-	46 (N47_E41390)

Gene expression detected by transcriptome and mass spectroscopy proteome analysis of the TRIP culture grown on phenanthrene are expressed as read counts (fragments per kilobase of gene per million mapped reads) and number of unique peptides identified over runs performed on four independent samples respectively.

Table S1). Such enzymes generate precursors for the synthesis of nucleic acids and amino acids (Zubay, 1983).

The genome further contains genes for the subunits of a pyruvate dehydrogenase complex required for transforming pyruvate into acetyl-CoA. All sequence analysis including similarities, synteny and protein domain predictions (Médigue *et al*., 2017) pointed to the classification of the aforementioned genes as encoding a 2-oxo-acid dehydrogenase and not a 2-oxo-acid:ferredoxin oxidoreductase. This excludes the possibility of producing reduced ferredoxin at this step which is needed for reduction of the ring system in anaerobic naphthalene degradation by Deltaproteobacterium N47 (Weyrauch, unpublished results). Expression of the pyruvate dehydrogenase complex was detected both by transcriptomics and proteomics (Fig. 4 and Supporting Information Table S1).

For oxidation of acetyl-CoA, genes for a complete tricarboxylic acid (TCA) cycle (citrate synthase, isocitrate dehydrogenase, succinyl-CoA synthetase, succinate dehydrogenase, fumarate hydratase and malate dehydrogenase) were detected, with the exception of 2-oxoglutarate dehydrogenase. Instead, the cycle is closed by a 2-oxoglutarate:ferredoxin oxidoreductase. Expression of the genes encoding the aforementioned enzymes was detected during growth of the TRIP culture with phenanthrene (Fig. 4 and Supporting Information Table S1). The substitution of 2-oxoglutarate dehydrogenase by 2-oxoglutarate:ferredoxin oxidoreductase is well documented in microaerophilic and strictly anaerobic organisms (Spormann and Thauer, 1989; Yun *et al.,* 2001). The reaction generates reduced ferredoxin, which can provide low-potential electrons for aryl-CoA reductases, required for anaerobic degradation of aromatic compounds (Bergmann *et al.,* 2011a,b). Moreover, the participation of 2-oxoglutarate:ferredoxin oxidoreductase has been previously demonstrated during the anaerobic degradation of naphthalene by Deltaproteobacteria N47 and NaphS2 (Weyrauch, unpublished results). 2-oxoglutarate:ferredoxin oxidoreductase is known as a key enzyme in the reductive TCA cycle, which is used by some bacteria for carbon fixation (Buchanan and Arnon, 1990). Two other key enzymes of the reductive TCA-cycle are the fumarate reductase and ATP citrate lyase. However, only genes for the fumarate reductase could be unambiguously detected in the genome of candidate *Desulfatiglans* TRIP_1 (Fig. 4 and Supporting Information Table S1). It cannot be excluded that the absence of the ATP citrate lyase in the genome of TRIP1 is due to genome incompleteness, as an estimated 0.7% of the genome is missing (Table 1). Nonetheless, lack of the ATP citrate lyase would not exclude the possibility of candidate *Desulfatiglans* TRIP_1 to run a reductive TCA cycle, as some citrate synthases have been reported to

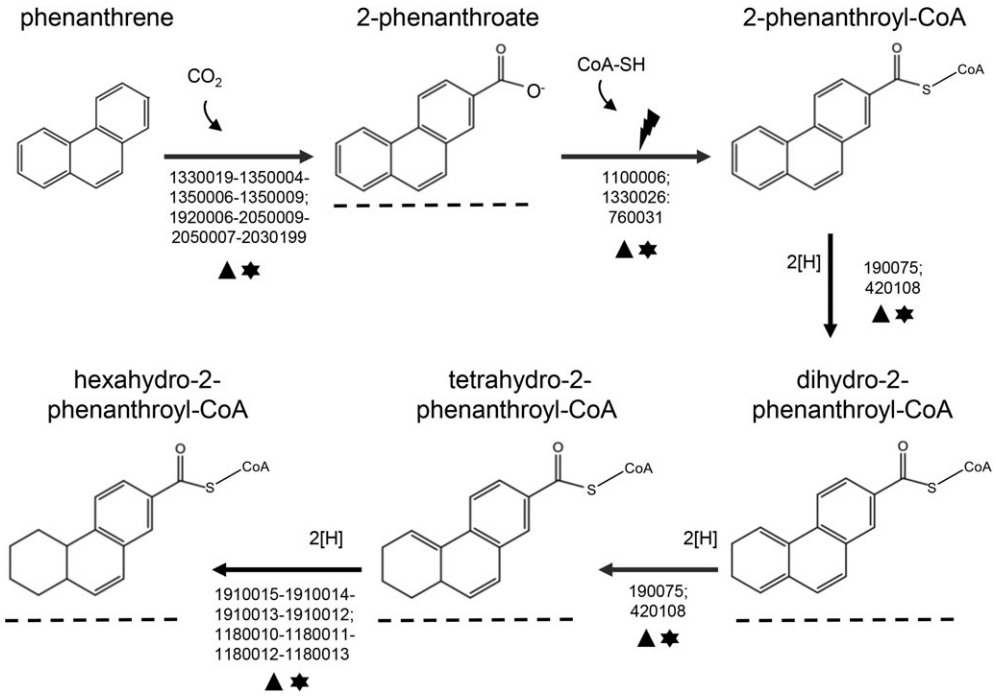

Fig. 3. Proposed phenanthrene degradation pathway in candidate *Desulfatiglans* TRIP_1.
Names below the arrows indicate the genes identified in the genome of this bacteria potentially involved in the respective reaction. Stars indicate that gene expression was detected by proteomic analyses, whereas triangles indicate that gene expression was detected by transcriptomics. Lightning bolt and underline compounds represent enzymatic activity and metabolites detected by Himmelberg *et al*., 2018 respectively.

perform the reverse reaction similar to the ATP citrate lyase (Mall *et al*., 2018). Hence, candidate *Desulfatiglans* TRIP_1 and the naphthalene-degrading Deltaproteobacterium N47 could resemble other sulfate-reducing bacteria such as *Desulfobacter hydrogenophilus*, which have the potential to switch between a hetero-organotrophic metabolism of growth using the TCA cycle for complete acetate oxidation and a litho-autotrophic metabolism of growth, with H_2, CO_2 and sulfate, assimilating CO_2 to acetate using the reductive TCA cycle (Schauder *et al.,* 1987; Bergmann *et al.,* 2011b). In fact, the genome of candidate *Desulfatiglans* TRIP_1 contains a gene encoding a NiFe Group 3 hydrogenase which catalyses hydrogen oxidation according to the HydDB classification system (Søndergaard *et al*., 2016), as well as genes for sulfide oxidation. However, the products of these genes were not detected in the proteomic analysis of the TRIP culture grown with phenanthrene as substrate (Fig. 4 and Supporting Information Table S1).

In addition to a complete TCA cycle, candidate *Desulfatiglans* TRIP_1 presents and expresses the genes for a Wood-Ljungdahl pathway (Wood *et al*., 1986), including the carbon monoxide dehydrogenase/acetyl coenzyme A (CoA) synthetase enzyme complex (Fig. 4 and Supporting Information Table S1). Many sulfate reducers are known to use the reversed Wood–Ljungdahl pathway for the oxidation of acetyl-CoA to CO_2 (Spormann and Thauer, 1989; Strittmatter *et al*., 2009), which suggests that candidate *Desulfatiglans* TRIP_1 both harbours and simultaneously expresses two pathways for the complete oxidation of acetyl-CoA during growth on phenanthrene. The implications of a joint expression of the Wood-Ljungdahl pathway and TCA cycle are still elusive, even though this has been previously observed for other PAH-degrading bacteria such as the sulfate reducer Deltaproteobacterium N47 (Bergmann *et al*., 2011b).

Candidate *Desulfatiglans* TRIP_1 expressed the genes for a NADH dehydrogenase complex, as well as for a succinate dehydrogenase/fumarate reductase complex needed for a potential electron transport chain. The genome also contains several genes encoding cytochromes, including a cytochrome bd complex and two gene clusters encoding subunits of a F0-F1 ATP synthase (Fig. 4 and Supporting Information Table S1).

The genome of candidate *Desulfatiglans* TRIP_1 also contains genes encoding acetate kinase, phosphate acetyltransferase and lactate dehydrogenase which were detected by both proteomic and transcriptomic analyses (Supporting Information Table S1). However, even though a fermentative lifestyle with less reduced substrates cannot be excluded for candidate *Desulfatiglans* TRIP_1, the TRIP culture was neither able to grow with phenanthrene without a terminal electron acceptor, nor is

this thermodynamically feasible under standard conditions (Himmelberg *et al*., 2018).

Enzymes for the anaplerotic reactions required to replenish intermediates of the TCA cycle: acetyl-CoA synthetase, pyruvate synthase, phosphoenolpyruvate synthase and phosphoenolpyruvate carboxykinase are encoded in the genome of candidate *Desulfatiglans* TRIP_1 (Fig. 4 and Supporting Information Table S1). This genome also encodes all the genes required for nucleotide anabolism and for the synthesis of 18 of the 20 essential amino acids, suggesting auxotrophy for the amino acids methionine and tyrosine. Enzymes for the synthesis of the unsaturated fatty acids palmitoleate, cis-vaccenate and (5Z)-dodec-5-enoate, and for the synthesis of diacylglycerol and the glycerophospholipids phosphatidylglycerol and phosphatidylethanolamine are encoded in the genome of candidate *Desulfatiglans* TRIP_1. Moreover, genes were found for the synthesis of the lipopolysaccharides 3-deoxy-D-manno-oct-2-ulosonic acid and GDP-D-glycero-α-D-manno-heptose. This organism

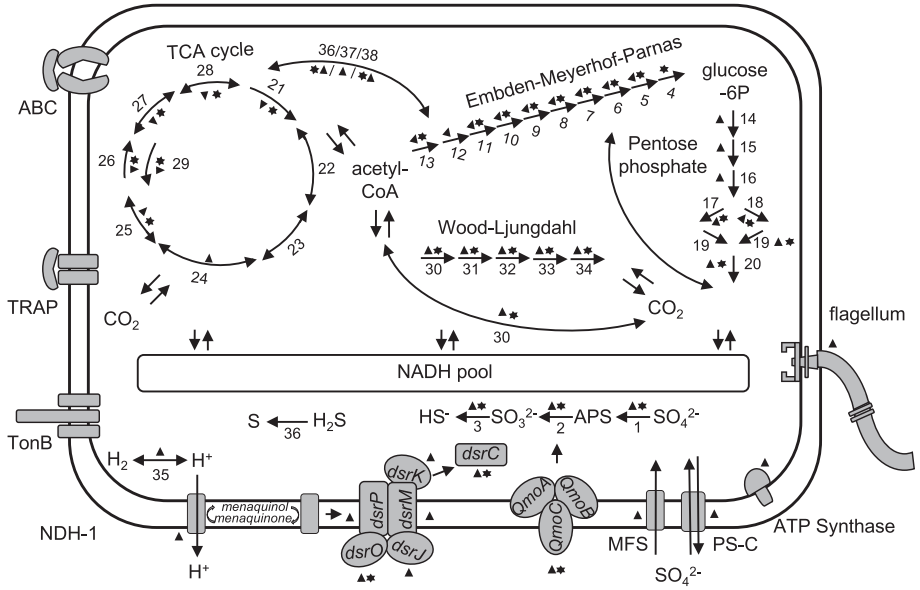

Fig. 4. Metabolic pathways, membrane transporters and mobility machinery of candidate *Desulfatiglans* TRIP_1 predicted by genomic analysis. Stars represent that gene expression was detected by proteomics, whereas triangles represent gene expression was detected by transcriptomics. Enzymes and corresponding genes of candidate *Desulfatiglans* TRIP_1 are **1**: sulfate adenylyltransferase/ATP-sulfurylase (PITCH_v1_a640025, PITCH_v1_a890006); **2**: adenylylsulfate reductase (PITCH_v1_a420043, PITCH_v1_a420042); **3**: sulfite reductase, dissimilatory-type (PITCH_v1_a1920018, PITCH_v1_a1920019); **4**: glucosephosphate isomerase (PITCH_v1_a2160001); **5**: fructose-1,6-bisphosphatase (PITCH_v1_a360022); **6**: fructose-bisphosphate aldolase (PITCH_v1_a650001, PITCH_v1_a1100020); **7**: triosephosphate isomerase (PITCH_v1_a1430023); **8**: glyceraldehyde-3-phosphate dehydrogenase (PITCH_v1_a1530016, PITCH_v1_a650002); **9**: phosphoglycerate kinase (PITCH_v1_a1430002); **10**: phosphoglycerate mutase (PITCH_v1_a420011, PITCH_v1_a1740051); **11**: enolase (PITCH_v1_a650014); **12**: phosphoenolpyruvate synthase (PITCH_v1_a230144; PITCH_v1_a2030037); **13**: pyruvate dehydrogenase (PITCH_v1_a140024, PITCH_v1_a140025, PITCH_v1_a140026); **14**: glucose-6-phosphate-1-dehydrogenase (PITCH_v1_a290049); **15**: 6-phosphogluconolactonase (PITCH_v1_a290051); **16**: 6-phosphogluconate dehydrogenase (PITCH_v1_a290048); **17**: ribose-5-phosphate isomerase (PITCH_v1_a850015); **18**: ribulose-5-phosphate 3-epimerase (PITCH_v1_a840039); **19**: transketolase (PITCH_v1_a780088); **20**: transaldolase (PITCH_v1_a190158); **21**: citrate synthase (PITCH_v1_a1880007); **22**: aconitase (PITCH_v1_a290047); **23**: isocitrate dehydrogenase (PITCH_v1_a290046); **24**: 2-oxoglutarate ferredoxin oxidoreductase (PITCH_v1_a950014, PITCH_v1_a950015, PITCH_v1_a950016); **25**: succinyl-CoA synthetase (PITCH_v1_a33002, PITCH_v1_a330022); **26**: succinate dehydrogenase (PITCH_v1_a2230003, PITCH_v1_a2230004, PITCH_v1_a220030), **27**: fumarate hydratase (PITCH_v1_a2030213, PITCH_v1_a2030214), **28**: malate dehydrogenase (PITCH_v1_a1070028); **29**: fumarate reductase (PITCH_v1_a220030, PITCH_v1_a220031, PITCH_v1_a220032); **30**: bifunctional carbon monoxide dehydrogenase/acetyl-CoA synthase (PITCH_v1_a190091, PITCH_v1_a190092, PITCH_v1_a190093, PITCH_v1_a190094); **31**: methylenetetrahydrofolate reductase (PITCH_v1_a190056, PITCH_v1_a1120007, PITCH_v1_a640013, PITCH_v1_a1120002, PITCH_v1_a720054); **32**: methylenetetrahydrofolate dehydrogenase-methenyltetrahydrofolate cyclohydrolase (PITCH_v1_a520030); **33**: formate-tetrahydrofolate ligase (PITCH_v1_a510003); **34**: formate dehydrogenase (PITCH_v1_a780006, PITCH_v1_a780004, PITCH_v1_a880015, PITCH_v1_a880017); **35**: hydrogen dehydrogenase (PITCH_v1_a80017); sulfide dehydrogenase (PITCH_v1_a890054, PITCH_v1_a890055, PITCH_v1_a520040, PITCH_v1_a520041); **36**: acetyl-CoA synthetase (PITCH_v1_a780099, PITCH_v1_a1780003, PITCH_v1_a140027, PITCH_v1_a1780001); **37**: pyruvate synthase (PITCH_v1_a2030096, PITCH_v1_a2030097), **38**: phosphoenolpyruvate carboxykinase (PITCH_v1_a190066). MFS: major facilitator superfamily transporter (PITCH_v1_a890040); PS-C: protons/sulfate cotransporter (PITCH_v1_a760059); DsrC: dissimilatory sulfite reductase complex associated protein (PITCH_v1_a1920015); DsrPOJKM redox complex associated to dissimilatory sulfite reductase (PITCH_v1_a220024, PITCH_v1_a220025, PITCH_v1_a220026, PITCH_v1_a220027, PITCH_v1_a220028); QmoABC: quinone-interacting membrane bound oxidoreductase (PITCH_v1_a420045, PITCH_v1_a420046, PITCH_v1_a420047). NDH-1: NADH-quinone oxidoreductase (PITCH_v1_a1120003, PITCH_v1_a1120004, PITCH_v1_a1120005, PITCH_v1_a1260030, PITCH_v1_a1260031, PITCH_v1_a1260032, PITCH_v1_a1260034, PITCH_v1_a1260035, PITCH_v1_a1260036, PITCH_v1_a1260037, PITCH_v1_a1260038, PITCH_v1_a1260039, PITCH_v1_a1260040, PITCH_v1_a1260041, PITCH_v1_a1260042). ABC: ATP-binding cassette transporters, TRAP: tripartite ATP-independent transporters.

appears able to Synthesize the following vitamins and cofactors: thiamine, riboflavin, pyridoxine, nicotinate, nicotinamide, pantothenic acid, biotin, folate, coenzyme A, guanylyl molybdenum cofactor and cobalamin (not shown).

Additionally, the genome harbours 67 genes for different transporter systems, including ATP-binding cassette (ABC) transporters, tripartite ATP-independent periplasmic transporters (TRAP), energy-coupling factor (ECF) transporters and Tol/Ton-dependent transporters, as well as 46 genes encoding secretion systems. The expression of a subset of these genes was detected by proteomics and/or transcriptomics (Fig. 4 and Supporting Information Table S1). Although no ABC transporter system for sulfate could be found, two genes encoding sulfate transporters were present, one belonging to the Major Facilitator Superfamily (Pao *et al*., 1998) and a probable proton/sulfate cotransporter (Fig. 4 and Supporting Information Table S1). TonB-dependent transporters have been reported for the uptake of aromatic compounds in some bacteria (Miller *et al*., 2010). Multiple gene clusters containing proteins associated to TonB-dependent transport systems were identified in the genome of candidate *Desulfatiglans* TRIP_1 (Fig. 4 and Supporting Information Table S1). Hence, it is possible that candidate *Desulfatiglans* TRIP_1 uses TonB-dependent transporters for phenanthrene uptake. On the other hand, PAHs can enter bacterial cells through passive diffusion. Furthermore, proton motive force-dependent transport mechanism of Gram-negative bacteria has been reported (Hua *et al*., 2004). Two genes encoding such proteins were identified in the genome of candidate *Desulfatiglans* TRIP_1, one being part of the putative phenanthrene carboxylase gene cluster. Expression of these two genes was detected during the transcriptomic assay (Table 3 and Supporting Information Table S1).

Moreover, 43 genes encoding flagella structure and regulation proteins, as well as 28 genes encoding chemotaxis proteins were identified, suggesting that candidate *Desulfatiglans* TRIP_1 has chemotactic sensing abilities. Most of these genes were detected in the transcriptomic analysis of the TRIP culture, but were absent from the proteomic data (Fig. 4 and Supporting Information Table S1).

Finally, the genome of candidate *Desulfatiglans* TRIP_1 harbours genes annotated as benzylsuccinate synthase, which is the first enzyme in the anaerobic toluene degradation pathway. These genes share between 40% and 50% sequence identity to those encoding the subunits of naphthyl-2-methyl-succinate synthase of Deltaproteobacterium N47 (Bergmann *et al.,* 2011a), the first enzyme in the anaerobic degradation of 2-methylnaphtalene, suggesting that this glycyl radical enzyme could be involved in the anaerobic degradation of methylphenanthrene. Consistently, these genes were not expressed during growth with phenanthrene (Supporting Information Table S1).

The other four nearly complete genomes of the TRIP culture also carry the genes for the Emden-Meyerhof-Parnas pathway (Table 6), the TCA cycle and at least one branch of the pentose phosphate pathway. Moreover, all bacteria encode at least one pathway for enabling a fermentative metabolism. Genes necessary for dissimilatory sulfate reduction were only present in the two candidate *Desulfatiglans* genomes. These two bacteria, as well as the candidate *Zixibacterium* present at least one putative CO_2 fixation pathway. The candidate *Zixibacterium* also possesses genes for denitrification, candidate *Desulfatiglans* TRIP_2 possesses genes for thiosulfate disproportionation and candidate *Paludibacter* TRIP_3 genes for nitrogen fixation (Table 6).

As aforementioned, we did not find potential genes encoding enzymes directly involved in phenanthrene degradation in the non-dominant genomes of the TRIP culture. A potential role in phenanthrene degradation of the four microorganisms other than candidate *Desulfatiglans* TRIP_1 could thus only be indirect. The genome of candidate *Spirochaetaceae* TRIP_4 suggests metabolic capacities similar to *Rectinema cohabitans.* The rod-shape Spirochaete *R. cohabitan*s was isolated from the naphthalene-degrading enrichment culture N47 where it is involved in necromass recycling providing hydrogen and possibly nutrients to the naphthalene-degrading Deltaproteobacterium N47 (Dong *et al*., 2018). Although the genetic elements for hydrogen transfer between the candidate *Spirochaetaceae* TRIP_4 and the candidate *Desulfatiglans* TRIP_1 are present, the corresponding gene products were not detected durig growth of the TRIP culture with phenanthrene. This includes a [NiFe] hydrogenase in candidate *Desulfatiglans* TRIP_1 (Supporting Information Table S1) and four genes encoding [FeFe] hydrogenases, as well as genes required for fermentation of carbohydrates in candidate *Spirochaetaceae* TRIP_4 (Table 6). *Paludibacter* species related to candidate *Paludibacter* TRIP_3 have also been reported in PAHs-contaminated sites (Yang *et al*., 2016). Also these microorganisms are able to grow with dead biomass, which could explain their persistance in the TRIP culture (Yang *et al*., 2016).

When we compared the contribution of each of the members of the TRIP culture to the N, C, S and Fe cycles using the MEBS (Multigenomic Entropy-Based Score) software (De Anda *et al*., 2017), none of the members of the TRIP culture showed a predominant role in any of the biogeochemical cycles. However, candidate *Zixibacteria* TRIP_5 presented a comparatively higher score for the iron cycle (not shown), mostly based on cytochromes b and c as well putative iron-siderophore transporters.

The multiomics metabolic reconstruction suggests that candidate *Desulfatiglans* TRIP_1 is the the primary producer of biomass in the culture and the only phenanthrene

Table 6. Metabolic potentialities of the bacteria constituting the TRIP culture according to genome analysis.

Metabolic pathway	*Desulfatiglans* TRIP_1	*Desulfatiglans* TRIP_2	*Paludibacter* TRIP_3	*Spirochaetaceae* TRIP_4	*Zixibacteria* TRIP_5
Embden-Meyerhof-Parnas pathway	Δ *	*	Δ *		
Acetyl-CoA biosynthesis (acetate)					
Acetyl-CoA biosynthesis (pyruvate)			Δ		
Pentose phosphate pathway (non-oxidative)	Δ *				
Pentose phosphate pathway (oxidative)					
TCA cycle	Δ *	*	Δ		
Wood–Ljungdahl pathway	Δ *	*			
Reductive monocarboxylic acid cycle					
Pyruvate fermentation to acetate	Δ *				
Pyruvate fermentation to ethanol					
Pyruvate fermentation to lactate					
Dissimilatory Sulfate reduction	Δ *	Δ *			
Sulfur reduction	Δ	*			*
Sulfide oxidation					
Thiosulfate disproportionation					
Nitrate reduction					
Hydrogen production		*			
Hydrogen oxidation		*			
Benzoate degradation					
Benzoyl-CoA degradation	Δ *	*			
Toluene degradation	Δ				
Ethanol degradation	Δ *				
Glycerol degradation					
Nitrogen fixation					
Ammonia assimilation					

Complete pathways encoded in the respective genome are indicated in grey. Asterisks represent that gene expression was detected by proteomics, whereas triangles represent gene expression was detected by transcriptomics.

degrader with sulfate as electron acceptor. The other abundant members are most likely necromass degraders recycling dead biomass with a fermentative lifestyle.

Conclusion

For the first time, this work describes genes involved in the anaerobic degradation of the three-ring PAH phenanthrene. Our results show that the anaerobic degradation of phenanthrene follows the same biochemical principles known for the anaerobic degradation of the model two-ring PAH naphthalene, i.e. an initial activation of phenanthrene by carboxylation and CoA ligation followed by a stepwise ring reduction by type III and type I aryl-CoA reductases. Subsequently, the pathway proceeds by ß-oxidation-like reactions and hydrolytic ring cleavage. The predominant microorganism in the TRIP culture, candidate *Desulfatiglans* TRIP_1 most likely performs the complete degradation of phenanthrene whereas the other members of the TRIP culture are involved in secondary degradation of necromass.

Experimental procedures

Cultivation of the TRIP enrichment culture

The TRIP culture was enriched from the Pitch Lake in Trinidad-Tobago (Himmelberg *et al*., 2018) and was grown anaerobically in carbonate-buffered freshwater mineral medium (Widdel and Bak, 1992) at 30 °C in the dark. Sulfate (10 mM) was added as terminal electron acceptor and 1.5% w/v phenanthrene in a liquid carrier phase (2,2,4,4,6,8,8-heptamethylnonane) was used as carbon source. Cultures were transferred (10% v/v) to fresh medium every 8–10 weeks.

DNA extraction

The TRIP culture was grown as described above until middle exponential phase. Cells were harvested by centrifugation (20 min, 6000 × g, 4 °C) and DNA was extracted using the DNeasy™ Blood and Tissue Kit (Qiagen).

Metagenome analysis

The metagenome of the TRIP culture was sequenced (Illumina PE 250 on MiSeq) and genome-resolved analyses of the raw shotgun data were performed (Himmelberg *et al*., 2018). The preassembly protocol followed the steps described in (Gkanogiannis *et al*., 2016) and the Spades engine (Bankevich *et al*., 2012) was used for targeted assemblies. The resulting scaffolds were annotated using the MicroScope microbial genome annotation and analysis platform (Médigue *et al*., 2017).

The genome sequence of candidate *Desulfatiglans* TRIP_1 has been submitted to the ENA databases and can be accessed under contig accession numbers: LT984854-LT984881.

MicroScope's syntactic annotation pipeline was used to identify protein coding genes, transfer RNA (tRNA), ribosomal RNA (rRNA), noncoding RNA (ncRNA) and repeat elements. Functional annotations were derived using generalist protein sequence (UniProtKB/Swiss-Prot), protein domain (Interpro, FIGFAM) and metabolic databases (KEGG, MetaCyc).

Completeness of genomic sequence

The completeness and contamination levels of the reconstructed bacterial genomes were evaluated with the checkM software (Parks *et al.,* 2015), based on the distribution pattern of a set of ubiquitous and single-copy marker genes within a reference genome tree.

Microorganisms relative abundance

The relative abundance of the bacteria composing the TRIP culture was estimated by re-mapping the raw reads to the assembled scaffolds using the BWA software (Li and Durbin, 2009), and the estimates were confirmed by 16S rRNA gene amplicon sequencing. For the latter, the V3-V4 region of the 16S rRNA gene was amplified from the DNA of the TRIP culture and used for library construction. PCR products were converted into blunt ends using T4 DNA polymerase Klenow Fragment and T4 Polynucleotide Kinase previous to adaptor addition. After quality control, libraries were sequenced (Illumina PE 250 on MiSeq 2500). The raw data were filtered to eliminate adapters and low-quality calls to obtain clean reads. Overlapping paired-end reads were merged and clustered into operational taxonomic units (OTUs) using MetaAmp Version 2.0 (Dong *et al.,* 2017). Amplicon sequences have been submitted to the GenBank database and can be accessed under accession number PRJNA479783.

Phylogenetic analysis

The full-length 16S rRNA gene sequences of the organisms from the TRIP culture were compared with the SILVA (Quast *et al.,* 2013) and NCBI (Benson *et al.,* 2012) databases.

Metabolic reconstruction

The metabolic capabilities of the different microorganisms were predicted from their genome using the KEGG (Kanehisa and Goto, 2000) and MetaCyc (Caspi *et al.,* 2016) databases; followed by a manual curation of the predicted pathways. Candidate genes relevant for PAH degradation were identified by homology to previously characterized enzymes involved in the anaerobic degradation of naphthalene using the blastp program (Altschul *et al.,* 1990).

Metatranscriptome analyses

The TRIP culture was grown as described above and cells were harvested in the mid-exponential phase by centrifugation (20 min, 6000 × g, 4 °C). Total RNA was immediately extracted using the Trizol™ reagent (Invitrogen). Samples were treated with the DNA-free™ kit (Invitrogen) to remove DNA. After rRNA depletion, the mRNA was used for strand-specific library construction and sequencing (Illumina PE100 in Hiseq 4000).

The raw RNA-seq reads were filtered to remove adapter sequences, contamination and low-quality reads. After quality control, the metatranscriptomic reads were mapped against the reconstructed genomes using bowtie2 (Langmead and Salzberg, 2012). Gene expression levels were estimated from the abundance of mapped reads using the featureCounts software (Liao *et al.,* 2014), with results expressed as fragments per kilobase of gene per million mapped reads. The transcriptome sequences of the TRIP culture grown in phenanthrene have been submitted to the GenBank database and can be accessed under accession number PRJNA479783.

Mass spectroscopy

Sample preparation

Cells were harvested by centrifugation in the mid-exponential growth phase (20 min, 6000 × g, 4 °C) and immediately frozen at −20 °C. The frozen cell pellets were warmed to room temperature and taken up in phosphate buffered saline (PBS buffer, pH 7.4). Cells were lysed by ultrasonification in a Bioruptor® (Diagenode) for 5 min to release the proteome and shear the genomic DNA. Samples were centrifugated (5 min, 12 000 × g, 4 °C) and supernatants were transferred to fresh 1.5 ml Eppendorf tubes. The protein concentration was determined using a modified Bradford assay (Ernst and Zor, 2010). An aliquot corresponding to 30 μg total protein per sample was removed and taken up in 2% v/v SDS and subsequently reduced with 5 mM DTT for 5 min at 90 °C. Next, reduced proteins were alkylated with 20 mM iodoacetamide (IAM) for 30 min at room temperature in the dark. Reduced and alkylated proteins were then subjected to methanol/chloroform precipitation (Wessel and Flügge, 1984). The protein pellets were then taken up in 50 μl 8 M Urea and 100 mM ammonium bicarbonate (ABC) and cleared by centrifugation (30 s; 10 000 × g).

Clear solutions of 25 μl (corresponding to 15 μg total protein) were transferred to fresh Eppendorf tubes, supplemented with 500 ng LysC (ratio 1/30) and incubated at 37 °C for 3 h while vigorously shaking. Samples were diluted with 100 mM ABC until the urea concentration was below 1 M. Then 1 μg Trypsin was added (ration 1/15) and the samples incubated over night at 37 °C while vigorously shaking. The digestion was stopped the next morning by adding formic acid (final concentration 5% v/v).

Sample clean-up for LC–MS

Acidified tryptic digests were desalted on home-made C18 StageTips as previously described (Rappsilber *et al*., 2007). On each 2 disc StageTip around 15 μg peptides were loaded (based on the initial protein concentration). After elution from the StageTips, samples were dried using a vacuum concentrator (Eppendorf) and the peptides were taken up in 10 μl 0.1% v/v formic acid solution.

LC–MS/MS

Experiments were performed on an Orbitrap Elite instrument (Thermo, Michalski *et al*., 2012) that was coupled to an EASY-nLC 1000 liquid chromatography (LC) system (Thermo). The LC was operated in the one-column mode. The analytical column was a fused silica capillary (75 μm × 35 cm) with an integrated PicoFrit emitter (New Objective) packed in-house with Reprosil-Pur 120 C18-AQ 1.9 μm resin (Dr. Maisch). The analytical column was encased by a column oven (Sonation) and attached to a nanospray flex ion source (Thermo). The column oven temperature was adjusted to 45 °C during data acquisition. The LC was equipped with two mobile phases: solvent A (0.1% v/v formic acid, FA, in water) and solvent B (0.1% v/v FA in acetonitrile, ACN). All solvents were of ultra-high-performance liquid chromatography grade (Sigma). Peptides were directly loaded onto the analytical column with a maximum flow rate that would not exceed the set pressure limit of 980 bar (usually around 0.5–0.8 μl min^{-1}). Peptides were subsequently separated on the analytical column by running a 140 min gradient of solvent A and solvent B (start with 7% v/v B; gradient 7% to 35% v/v B for 120 min; gradient 35% to 100% v/v B for 10 min and 100% v/v B for 10 min) at a flow rate of 300 nl min^{-1}. The mass spectrometer was operated using Xcalibur software (version 2.2 SP1.48). The mass spectrometer was set in the positive ion mode. Precursor ion scanning was performed in the Orbitrap analyser (Fourier Transform Mass Spectrometry, FTMS) in the scan range of *m/z* 300–1800 and at a resolution of 60 000 with the internal lock mass option turned on (lock mass was 445.120025 *m/z*, polysiloxane, Olsen *et al*., 2005). Product ion spectra were recorded in a data dependent fashion in the ion trap (Ion Trap Mass Spectrometry, ITMS) in a variable scan range and at a rapid scan rate. The ionization potential (spray voltage) was set to 1.8 kV. Peptides were analysed using a repeating cycle consisting of a full precursor ion scan (1.0×10^6 ions or 30 ms) followed by 15 product ion scans (1.0×10^4 ions or 50 ms) where peptides are isolated based on their intensity in the full survey scan (threshold of 500 counts) for tandem mass spectrum (MS2) generation that permits peptide sequencing and identification. Collision-induced dissociation (CID) collision energy was set to 35% for the generation of MS2 spectra. During MS2 data acquisition, dynamic ion exclusion was set to 60 s with a maximum list of excluded ions consisting of 500 members and a repeat count of one. Ion injection time prediction, preview mode for the FTMS, monoisotopic precursor selection and charge state screening were enabled. Only charge states higher than 1 were considered for fragmentation.

Peptide and protein identification

Raw spectra were submitted to an Andromeda (Cox *et al*., 2011) search in MaxQuant (version 1.5.3.30) using the default settings (Cox and Mann, 2008). Label-free quantification and match-between-runs was activated (Cox *et al*., 2014). MS/MS spectra data were searched against the in-house generated databases of predicted proteins from candidate *Desulfatiglans* TRIP_1 (4868 entries), candidate *Desulfatiglans* TRIP_2 (4891 entries), candidate Zixibacteria TRIP_5 (3045 entries), candidate *Paludibacter* TRIP_3 (2636 entries) and candidate Spirochaetaceae TRIP_4 (2930 entries). All searches included also a contaminants database (as implemented in MaxQuant, 267 sequences). The contaminants database contains known MS contaminants and was included to estimate the level of contamination. Andromeda searches allowed oxidation of methionine residues (16 Da), acetylation of protein N-terminus (42 Da as dynamic modification) and the static modification of cysteine (57 Da, alkylation with IAM). Enzyme specificity was set to 'Trypsin/P' with two missed cleavages allowed. The instrument type in Andromeda searches was set to Orbitrap and the precursor mass tolerance was set to ±20 p.p.m. (first search) and ± 4.5 p.p.m. (main search). The MS/MS match tolerance was set to ±0.5 Da. The peptide spectrum match FDR and the protein FDR were set to 0.01 (based on target-decoy approach). Minimum peptide length was seven amino acids. For protein quantification, unique and razor peptides were allowed. Modified peptides were allowed for quantification. The minimum score for modified peptides was 40.

Data analysis

Initial data analysis was performed using the PERSEUS computational platform version 1.5.5.3 (Tyanova *et al*., 2016). The mass spectrometry proteomics data have been deposited to the ProteomeXchange Consortium via the PRIDE (Vizcaíno *et al*., 2016) partner repository (https://www.ebi.ac.uk/pride/archive/) with the dataset identifier PXD010151.

Acknowledgements

We acknowledge Xiyang Dong for his helpful advices on metabolic pathway reconstruction, and Alexander Probst (University of Duisburg-Essen) for advice during the analysis of transcriptomic data. We thank Karine Labadie and Eric Mahieu (Genoscope) for the shotgun sequencing of the TRIP metagenome, and Genoscope's LABGeM team for the creation and maintenance of the MicroScope annotation platform. This project has received funding from the European Union's Horizon 2020 research and innovation program under the Marie Sklodowska-Curie grant agreement No 705321 and from the ERC advanced grant EcOlLogy no. 666952.

References

Altschul, S.F., Gish, W., Miller, W., Myers, E.W., and Lipman, D.J. (1990) Basic local alignment search tool. *J Mol Biol* **215**: 403–410.

Bankevich, A., Nurk, S., Antipov, D., Gurevich, A.A., Dvorkin, M., Kulikov, A.S., *et al*. (2012) SPAdes: a new genome assembly algorithm and its applications to single-cell sequencing. *J Comput Biol* **19**: 455–477.

Benson, D.A., Cavanaugh, M., Clark, K., Karsch-Mizrachi, I., Lipman, D.J., Ostell, J., and Sayers, E.W. (2012) GenBank. *Nucleic Acids Res* **41**: D36–D42.

Bergmann, F.D., Selesi, D., and Meckenstock, R.U. (2011a) Identification of new enzymes potentially involved in anaerobic naphthalene degradation by the sulfate-reducing enrichment culture N47. *Arch Microbiol* **193**: 241–250.

Bergmann, F., Selesi, D., Weinmaier, T., Tischler, P., Rattei, T., and Meckenstock, R.U. (2011b) Genomic insights into the metabolic potential of the polycyclic aromatic hydrocarbon degrading sulfate-reducing Deltaproteobacterium N47. *Environ Microbiol* **13**: 1125–1137.

Buchanan, B.B., and Arnon, D.I. (1990) A reverse KREBS cycle in photosynthesis: consensus at last. *Photosynth Res* **24**: 47–53.

Cai, Q.Y., Mo, C.H., Wu, Q.T., Zeng, Q.Y., and Katsoyiannis, A. (2007) Occurrence of organic contaminants in sewage sludges from eleven wastewater treatment plants, China. *Chemosphere* **68**: 1751–1762.

Caspi, R., Billington, R., Ferrer, L., Foerster, H., Fulcher, C. A., Keseler, I.M., *et al*. (2016) The MetaCyc database of metabolic pathways and enzymes and the BioCyc collection of pathway/genome databases. *Nucleic Acids Res* **44**: D471–D480.

Cox, J., and Mann, M. (2008) MaxQuant enables high peptide identification rates, individualized p.p.b.-range mass accuracies and proteome-wide protein quantification. *Nat Biotechnol* **26**: 1367–1372.

Cox, J., Hein, M.Y., Luber, C.A., Paron, I., Nagaraj, N., and Mann, M. (2014) Accurate proteome-wide label-free quantification by delayed normalization and maximal peptide ratio extraction, termed MaxLFQ. *Mol Cell Proteomics* **13**: 2513–2526.

Cox, J., Neuhauser, N., Michalski, A., Scheltema, R.A., Olsen, J.V., and Mann, M. (2011) Andromeda: a peptide search engine integrated into the MaxQuant environment. *J Proteome Res* **10**: 1794–1805.

Davidova, I.A., Gieg, L.M., Duncan, K.E., and Suflita, J.M. (2007) Anaerobic phenanthrene mineralization by a carboxylating sulfate-reducing bacterial enrichment. *ISME J* **1**: 436–442.

De Anda, V., Zapata-Penasco, I., Poot-Hernandez, A.C., Equiarte, L.E., Contreras-Moreira, B., and Souza, V. (2017) MEBS, a software platform to evaluate large (meta)genomic collections according to their metabolic machinery: unraveling the sulfur cycle. *Gigascience* **6**: 1–17.

Di Donato, R.J., Young, N.D., Butler, J.E., Chin, K.J., Hixson, K.K., Mouser, P., *et al*. (2010) Genome sequence of the Deltaproteobacterial strain NaphS2 and analysis of differential gene expression during anaerobic growth on naphthalene. *PLoS One* **5**: e14072.

Dong, X., Greening, C., Brüls, T., Conrad, R., Guo, K., Blaskowski, S., *et al*. (2018) Fermentative Spirochaetes mediate necromass recycling in anoxic hydrocarbon-contaminated habitats. *ISME J* **12**: 2039–2050.

Dong, X., Kleiner, M., Sharp, C.E., Thorson, E., Li, C., Liu, D., and Strous, M. (2017) Fast and simple analysis of MiSeq amplicon sequencing data with MetaAmp. *Front Microbiol* **8**: 1461.

Eberlein, C., Estelmann, S., Seifert, J., von Bergen, M., Muller, M., Meckenstock, R.U., and Boll, M. (2013a) Identification and characterization of 2-naphthoyl-coenzyme a reductase, the prototype of a novel class of dearomatizing reductases. *Mol Microbiol* **88**: 1032–1039.

Eberlein, C., Johannes, J., Mouttaki, H., Sadeghi, M., Golding, B.T., Boll, M., and Meckenstock, R.U. (2013b) ATP-dependent/−independent enzymatic ring reductions involved in the anaerobic catabolism of naphthalene. *Environ Microbiol* **15**: 1832–1841.

Ernst, O., and Zor, T. (2010) Linearization of the Bradford protein assay. *J Vis Exp* **38**: 1918.

Estelmann, S., Blank, I., Feldmann, A., and Boll, M. (2015) Two distinct old yellow enzymes are involved in naphthyl ring reduction during anaerobic naphthalene degradation. *Mol Microbiol* **95**: 162–172.

Fuchs, G. (2008) Anaerobic metabolism of aromatic compounds. In *Incredible Anaerobes: From Physiology to Genomics to Fuels*, Vol. **1125**, Wiegel, J., Maier, R.J., and Adams, M.W.W. (eds). Oxford, UK: Blackwell Publishing, pp. 82–99.

Galushko, A., Minz, D., Schink, B., and Widdel, F. (1999) Anaerobic degradation of naphthalene by a pure culture of a novel type of marine sulphate-reducing bacterium. *Environ Microbiol* **1**: 415–420.

Gkanogiannis, A., Gazut, S., Salanoubat, M., Kanj, S., and Brüls, T. (2016) A scalable assembly-free variable

selection algorithm for biomarker discovery from metagenomes. *BMC Bioinformatics* **17**: 311.

Himmelberg, A.M., Brüls, T., Farmani, Z., Weyrauch, P., Barthel, G., Schrader, W., and Meckenstock, R.U. (2018) Anaerobic degradation of phenanthrene by a sulfate-reducing enrichment culture. *Environ Microbiol* **20**: 3589–3600.

Hua, Z.Z., Chen, Y., Du, G.C., and Chen, J. (2004) Effects of biosurfactants produced by *Candida Antarctica* on the biodegradation of petroleum compounds. *World J Microbiol Biotechnol* **20**: 4.

Kanehisa, M., and Goto, S. (2000) KEGG: Kyoto encyclopedia of genes and genomes. *Nucleic Acids Res* **28**: 27–30.

Langmead, B., and Salzberg, S.L. (2012) Fast gapped-read alignment with Bowtie 2. *Nat Methods* **9**: 357–359.

Li, H., and Durbin, R. (2009) Fast and accurate short read alignment with burrows-wheeler transform. *Bioinformatics* **25**: 1754–1760.

Liao, Y., Smyth, G.K., and Shi, W. (2014) featureCounts: an efficient general purpose program for assigning sequence reads to genomic features. *Bioinformatics* **30**: 923–930.

Mall, A., Sobotta, J., Huber, C., Tschirner, C., Kowarschik, S., Bačnik, K., *et al*. (2018) Reversibility of citrate synthase allows autotrophic growth of a thermophilic bacterium. *Science* **6375**: 563–567.

Meckenstock, R.U., Boll, M., Mouttaki, H., Koelschbach, J. S., Cunha Tarouco, P., Weyrauch, P., *et al*. (2016) Anaerobic degradation of benzene and polycyclic aromatic hydrocarbons. *J Mol Microbiol Biotechnol* **26**: 92–118.

Médigue, C., Calteau, A., Cruveiller, S., Gachet, M., Gautreau, G., Josso, A., *et al*. (2017) MicroScope-an integrated resource for community expertise of gene functions and comparative analysis of microbial genomic and metabolic data. *Brief Bioinform* **12**: 1–14.

Michalski, A., Damoc, E., Lange, O., Denisov, E., Nolting, D., Mueller, M., *et al*. (2012) Ultra high resolution linear ion trap Orbitrap mass spectrometer (Orbitrap Elite) facilitates top down LC MS/MS and versatile peptide fragmentation modes. *Mol Cell Proteomics* **11**: O111.013698.

Miller, T.R., Delcher, A.L., Salzberg, S.L., Saunders, E., Detter, J.C., and Halden, R.U. (2010) Genome sequence of the dioxin-mineralizing bacterium *Sphingomonas wittichii* RW1. *J Bacteriol* **192**: 6101–6102.

Mouttaki, H., Johannes, J., and Meckenstock, R.U. (2012) Identification of naphthalene carboxylase as a prototype for the anaerobic activation of non-substituted aromatic hydrocarbons. *Environ Microbiol* **14**: 2770–2774.

Olsen, J.V., de Godoy, L.M.F., Li, G., Macek, B., Mortensen, P., Pesch, R., *et al*. (2005) Parts per million mass accuracy on an Orbitrap mass spectrometer via lock mass injection into a C-trap. *Mol Cell Proteomics* **4**: 2010–2021.

Pao, S.S., Paulsen, I.T., and Saier, M.H., Jr. (1998) Major facilitator superfamily. *Microbiol Mol Biol Rev* **62**: 1–34.

Parks, D.H., Imelfort, M., Skennerton, C.T., Hugenholtz, P., and Tyson, G.W. (2015) CheckM: assessing the quality of microbial genomes recovered from isolates, single cells, and metagenomes. *Genome Res* **25**: 1043–1055.

Peng, R.H., Xiong, A.S., Xue, Y., Fu, X.Y., Gao, F., Zhao, W., *et al*. (2008) Microbial biodegradation of polyaromatic hydrocarbons. *FEMS Microbiol Rev* **32**: 927–955.

Pereira, I.A., Ramos, A.R., Grein, F., Marques, M.C., da Silva, S.M., and Venceslau, S.S. (2011) A comparative genomic analysis of energy metabolism in sulfate reducing bacteria and archaea. *Front Microbiol* **2**: 69.

Quast, C., Pruesse, E., Yilmaz, P., Gerken, J., Schweer, T., Yarza, P., *et al*. (2013) The SILVA ribosomal RNA gene database project: improved data processing and web-based tools. *Nucleic Acids Res* **41**: D590–D596.

Rappsilber, J., Mann, M., and Ishihama, Y. (2007) Protocol for micro-purification, enrichment, pre-fractionation and storage of peptides for proteomics using StageTips. *Nat Protoc* **2**: 1896–1906.

Schauder, R., Widdel, F., and Fuchs, G. (1987) Carbon assimilation pathways in sulfate-reducing bacteria II. Enzymes of a reductive citric acid cycle in the autotrophic *Desulfobacter hydrogenophilus*. *Arch Microbiol* **148**: 218–225.

Søndergaard, D., Pedersen, C.N.S., and Greening, C. (2016) HydDB: a web tool for hydrogenase classification and analysis. *Sci Rep* **6**: 34212.

Spormann, A.M., and Thauer, R.K. (1989) Anaerobic acetate oxidation to CO2 by *Desulfotomaculum acetoxidans*. *Arch Microbiol* **152**: 189–195.

Strittmatter, A.W., Liesegang, H., Rabus, R., Decker, I., Amann, J., Andres, S., *et al*. (2009) Genome sequence of *Desulfobacterium autotrophicum* HRM2, a marine sulfate reducer oxidizing organic carbon completely to carbon dioxide. *Environ Microbiol* **11**: 1038–1055.

Tyanova, S., Temu, T., Sinitcyn, P., Carlson, A., Hein, M.Y., Geiger, T., *et al*. (2016) The Perseus computational platform for comprehensive analysis of (prote)omics data. *Nat Methods* **13**: 731–740.

Vizcaíno, J.A., Csordas, A., del-Toro, N., Dianes, J.A., Griss, J., Lavidas, I., *et al*. (2016) 2016 update of the PRIDE database and related tools. *Nucleic Acids Res* **44**: D447–D456.

Wessel, D., and Flügge, U.I. (1984) A method for the quantitative recovery of protein in dilute-solution in the presence of detergents and lipids. *Anal Biochem* **138**: 141–143.

Widdel, F., and Bak, F. (1992) Gram-negative mesophilic sulfate-reducing bacteria. In *The Prokaryotes*, Balows, A., Trüper, H.G., Dworkin, M., Harder, W., and Schleifer, K.H. (eds). New York, NY: Springer.

Williams, R.E., and Bruce, N.C. (2002) "New uses for an old enzyme" – the old yellow enzyme family of flavoenzymes. *Microbiology* **148**: 1607–1614.

Wood, H.G., Ragsdale, S.W., and Pezacka, E. (1986) The acetyl-CoA pathway: a newly discovered pathway of autotrophic growth. *Trends Biochem Sci* **11**: 14–18.

Yang, S., Wen, X., Shi, Y., Liebner, S., Jin, H., and Perfumo, A. (2016) Hydrocarbon degraders establish at the costs of microbial richness, abundance and keystone taxa after crude oil contamination in permafrost environments. *Sci Rep* **6**: 37473.

Yun, N.R., Arai, H., Ishii, M., and Igarashi, Y. (2001) The genes for anabolic 2-oxoglutarate: ferredoxin oxidoreductase from *Hydrogenobacter thermophilus* TK-6. *Biochem Biophys Res Commun* **282**: 589–594.

Zhang, X., and Young, L.Y. (1997) Carboxylation as an initial reaction in the anaerobic metabolism of naphthalene and phenanthrene by sulfidogenic consortia. *Appl Environ Microbiol* **63**: 4759–4764.

Zubay, G. (1983) *Biochemistry*: Addison-Wesley Publishing Company, Inc., Menlo Park.

Supporting Information

Additional Supporting Information may be found in the online version of this article at the publisher's web-site:

Table S1. List of genes identified in the genome of candidate *Desulfatiglans* TRIP_1, classified according to their metabolic function. Gene expression detected by transcriptome and mass spectroscopy proteome analyses of the TRIP culture grown on phenanthrene are expressed as read counts (fragments per kilobase of gene per million mapped reads) and number of unique peptides identified over runs performed on four independent samples, respectively.